

Web-type silicon carbide fibers prepared by the electrospinning of polycarbosilanes

Dong-Geun Shin^{a,b}, Doh-Hyung Riu^{a,*} and Hyoun-Ee Kim^b

^aNanomaterials Team, Korea Institute of Ceramic Engineering and Technology, 233-5 Gasan-dong, Gueancheon-gu, Seoul 153-801, Korea

^bSchool of Materials Science and Engineering, Seoul National University, San 56-1 Shinrim-dong, Kwanak-gu, Seoul 151-742, Korea

Silicon carbide web was prepared by the electrospinning of polycarbosilane (PCS) solution and the pyrolysis of the electrospun web at 1000-1400 °C after a thermal curing process. The optimum spinning conditions for obtaining a uniform SiC web were a 1.3 g/ml PCS solution with 30% DMF/70% toluene composition and a spinning voltage higher than 20 kV. A uniform SiC web with fibers ranging from 1 to 3 μm was obtained. This was characterized by FE-SEM, infrared spectroscopy, thermogravimetric analysis, X-ray diffraction and transmission electron microscopy. A large amount of oxygen was introduced during the thermal curing of the as-spun web due to its large specific surface area; this resulted in an increased ceramic yield as the mixed phases of amorphous oxycarbide, SiC nanocrystallites, and amorphous silica. By increasing the pyrolysis temperature, this mixed phase underwent decomposition that made the fiber structure nanoporous.

Key words: SiC web, Electrospinning, Polycarbosilane, Solvent mixing ratio, Pyrolysis.

Introduction

Silicon carbide (SiC) is one of the well known nonoxide ceramics used as a high-temperature structural material. Various types of SiC, such as nanowire [1], thin film [2], foam [3], and continuous fiber [4-6] have been developed since the early 1980s and their applications have expanded into the military, aerospace, automobile, and electronics industries. In particular, SiC fiber is noteworthy for its use as reinforcement for high-temperature ceramic composites, substrates for catalysts, and high-temperature filters. Recently, several attempts have been made to study the applications of SiC fibers, such as for gas-fueled radiation heater [7], diesel particulate filter (DPF) [8, 9], and ceramic fiber separators [10, 11], for which the diameter-controlled nano/micro SiC fibers are anticipated to be potential materials.

One of the promising techniques to obtain this nano/micro grade of SiC fibers is the electrospinning method [12-16]. Electrospinning has been utilized for the preparation of nanofibers using various materials that include polymers [17], composites [18, 19], and ceramics [12-16]. Oxide-based ceramic nanofibers have been prepared by the electrospinning of a sol-gel solution and pyrolysis up to specified temperatures [12-14]. Recently, boron carbide fibers were also prepared by electrospinning using a polymer precursor, which is a novel method for the fabrication of ceramic fibers through an organic-to-inorganic conversion process using polymer precursors [15].

The electrospinning technique is also notable in that the fiber diameters of the electrospun web can be easily controlled over a scale of nanometres to micrometres by controlling the processing parameters such as the solution viscosity, solvent composition, and electric field [20]. We expect that the SiC fibers with an intermediate fiber diameter ranging from several hundreds of nanometres to micrometres will lead to new fields of application.

In this paper, we studied the fabrication of SiC fibers through the electrospinning of polycarbosilane (PCS); in particular, our studies were based on a SiC web that possesses fiber diameters of 1-3 μm, which is the intermediate range between a continuous fiber (~20 μm) and a nanofiber (~200 nm). The effects of the concentration of the polymer precursor solution, solvent mixing ratio, and electric field on the electrospinning process of PCS were investigated to obtain an SiC web with a uniform fiber diameter. The curing process, pyrolysis process, and the morphological evolution of the electrospun PCS fiber were also investigated.

Experimental Procedures

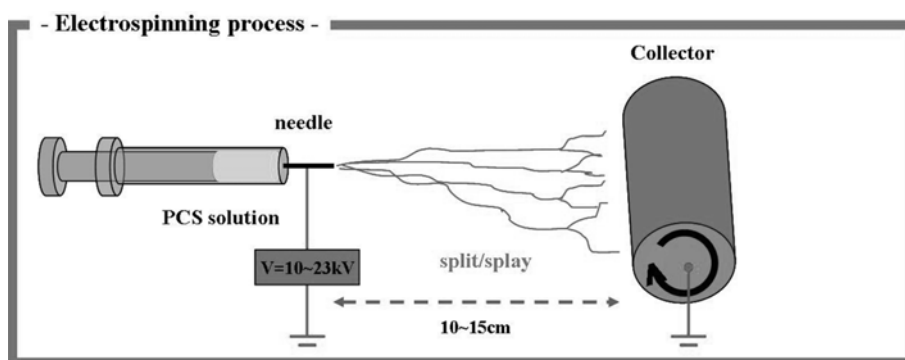
Polycarbosilanes (PCS, Nipusi Type A, Nippon Carbon Co., Japan) were selected as the precursors for the preparation of PCS web by electrospinning. Toluene and N,N-dimethylformamide (DMF) were purchased from Aldrich Company and used as the solvent for the PCS and the cosolvent for enhanced spinning performance, respectively. DMF was mixed with toluene in different ratios ranging from 0 to 50% by gentle stirring for 12 h at ambient temperature. Subsequently, PCS was added to the mixed solvent at various concentrations (0.6-1.5 g/ml)

*Corresponding author:
Tel : +82-2-3282-2497
Fax: +82-2-3282-7769
E-mail: dhriu15@kicet.re.kr

Table 1. Experimental conditions for the PCS solution

Solution condition		Fiber formation
Solvent composition (%DMF/Toluene)	Solution concentration (g/ml)	
0	1.2	△ (thick and sticky)
5	0.7	× (film formation)
5	1.0	× (drop)
5	1.1	△ (bead)
5	1.2	○ (bead)
5	1.3	○ (uniform)
5	1.5	× (nozzle clogging)
10	1.3	○ (uniform)
20	1.3	○ (uniform)
30	1.3	○ (uniform)
50	1.2	× (insoluble)

*Spinnability in naked eye: ○; very good, △; good, ×; bad

**Fig. 1.** Schematic illustration of the setup for the electrospinning process of the PCS/solvent solution.

and stirred for 24 h at room temperature in order to obtain a uniform solution. Table 1 shows the experimental conditions for the PCS solutions used for electrospinning.

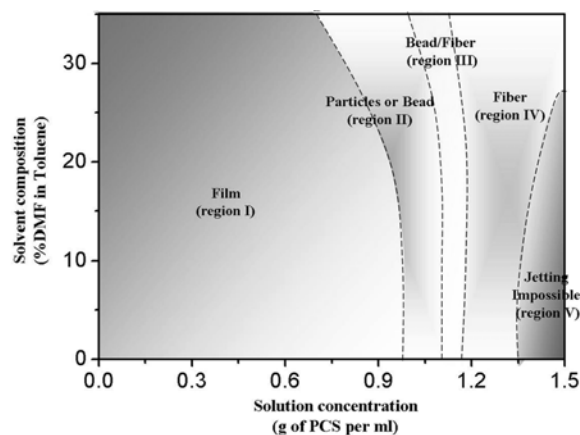
The electrospinning system comprises three parts: spinning part, collecting part, and power supply; this is schematically shown in Fig. 1. The PCS solution was loaded into a syringe with a capacity of 5 ml and subjected to electrospinning using a metallic needle with a diameter of 0.5 mm at a rate of 0.5 mm/h under an applied voltage in the range of 15–30 kV. The solution can be stretched without drop formation up to 23 kV. The distance between the needle tip and the collector that was covered with a metal mesh for easy separation of the fiber web was 100 mm. Samples with dimensions of 50 × 50 mm² were taken from the electrospun webs and subjected to thermal curing at 200 °C for 1 h in a muffle furnace and then pyrolyzed at 1000–1400 °C (100 °C/h) for 1 h under an argon atmosphere.

FT-IR spectroscopy (UV/IR-400 plus, Jasco, UK) and thermogravimetry analysis (TGA/SDTA 851, Mettler Toledo, U.S.A.) were used to analyze the pyrolysis behavior of the electrospun web. The fiber morphology was observed using FE-SEM (JSM-6700F, JEOL, Japan). Phase analysis was performed and microstructural evolution was determined using X-ray diffraction (XRD, FR-150, Enraf-Nonius

Co, Netherlands) and transmission electron microscopy (TEM, JEM-4010, JEOL, Japan).

Results and Discussions

Figure 2 shows the spinnability map for PCS solution with regard to the concentrations and solvent mixing ratios. The electrospinning behavior of the PCS solution was

**Fig. 2.** Spinnability map for the PCS solution prepared with different concentrations and solvent compositions.

classified into five regions: (1) the film region (region I) corresponds to the region of low concentration of PCS that takes any shape before the spinning jets reach the winder, (2) particles or beads region (region II) corresponds to a still lower PCS concentration, (3) beads/fiber transition region (region III) corresponds to the region in which the fibers are formed together with beads, (4) fiber region (region IV), and (5) jetting impossible region due to high viscosity (region V).

Without DMF in the solution, the region for the fiber formation corresponded to the concentration between 1.2 and 1.3 g/ml. Moreover, the fibers were thick and they stuck together when they arrived at the receiving drum. It is suggested that since the fibers were too thick for the solvent to diffuse out of the entire volume of the fiber; therefore, sufficient amount of solvent still remained that rendered the fibers to stick together. When only 5% of DMF was added, the fibers showed significantly smaller diameters and did not stick together. The fiber formation region became wider with further DMF addition. When the amount of DMF added was increased to over 20%, electrospinning was feasible between 1.0 and 1.5 g/ml.

Figure 3 shows the SEM images of the SiC webs

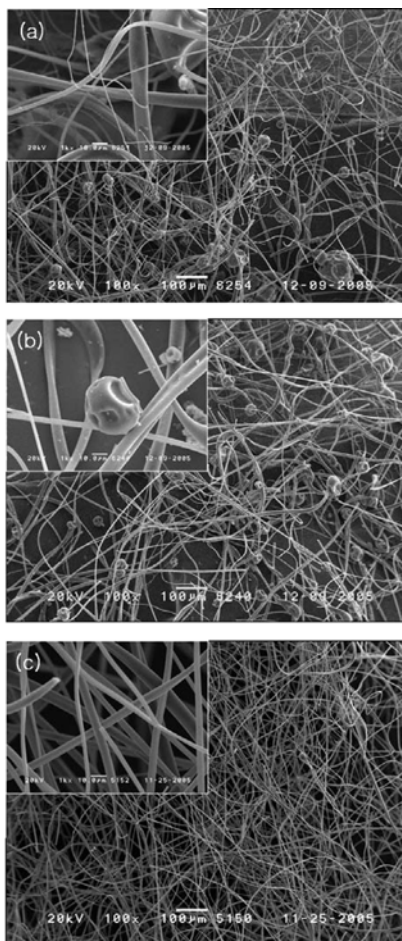


Fig. 3. SEM images of the SiC webs electrospun at the solution concentrations of (a) 1.1, (b) 1.2, and (c) 1.3 g/ml for 5% DMF/toluene mixed solvent.

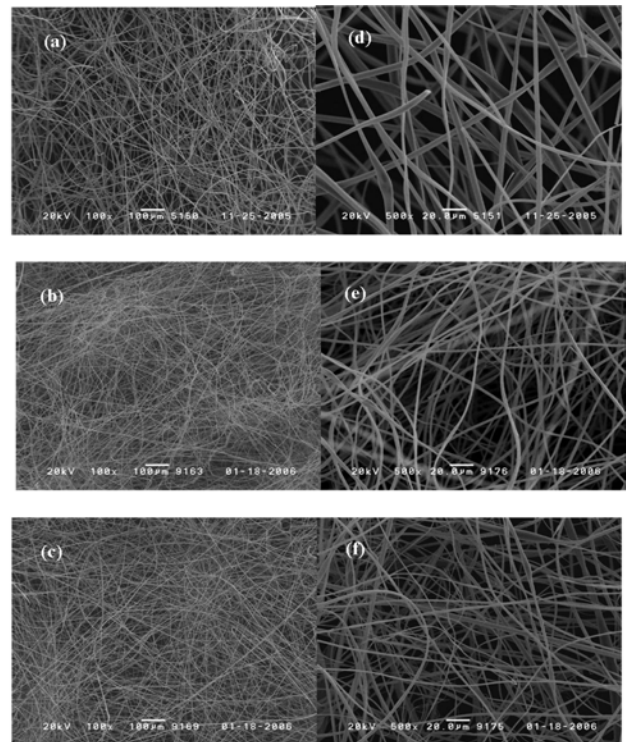


Fig. 4. SEM images of the SiC webs electrospun at the solvent compositions of (a) 5%, (b) 10%, and (c) 20% for a 1.3 g/ml solution.

prepared from various PCS concentrations in 5% DMF/toluene mixed solvent and pyrolyzed at 1200 °C. An SiC web with various fiber diameters and many beads was obtained at PCS concentrations lower than 1.2 g/ml. Beads are known to be formed frequently during the spinning of the less viscous solutions [21]. In general, the main factor for bead formation is the influence of surface tension [21, 22]. Beads are easily formed at low solution concentrations or for high evaporation rates of the solvent on the fiber surface, and they influence the degradation of the fiber-web qualities. The fiber diameter distribution became more uniform and the beads disappeared when the PCS concentration was 1.3 g/ml. However, a further increase in the PCS solution concentration above 1.3 g/ml was ineffective in reducing the fiber diameter. When the concentration was above 1.5 g/ml, electrospinning became impossible due to the high viscosity.

In order to reduce the fiber diameter, the solvent mixing ratio was further changed. Figure 4 shows the electrospun SiC webs prepared from the PCS solutions with a fixed concentration of 1.3 g/ml and the solvent mixing ratios (DMF/toluene) varying from 5 to 30%. With an increase in the DMF/toluene ratio, the fiber diameter of the SiC web decreased while maintaining a uniform fiber-diameter distribution. When the solvent mixing ratio was 30%, a uniform web with a fiber diameter ranging from 1.0 to 3.0 μm was obtained. DMF is a well known polyelectrolytic solvent with a low evaporation rate and high dielectric constant; hence, it was considered to be very effective in the elimination of beads with a reduction in the fiber

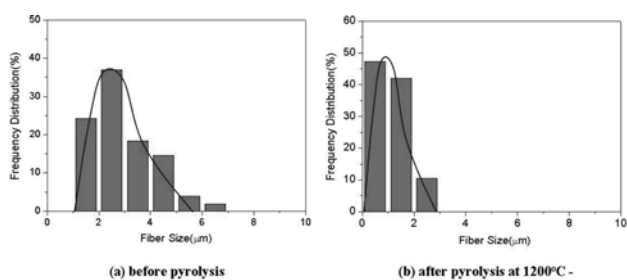


Fig. 5. Distribution of fiber diameters (a) before pyrolysis and (b) after pyrolysis at 1200 °C.

diameter [23, 25]. Figure 5 shows the distribution of the fiber diameters of the electrospun web prepared from the PCS solution with a concentration of 1.3 g/ml in 30% DMF/toluene solvent before and after pyrolysis at 1200 °C. The fiber diameter was directly measured from the SEM instrument using an image analysis program. The diameters of over 20 fibers were measured and the average values were 3.4 μm and 2.0 μm; this shows that the decrease in the diameter was approximately 40% after pyrolysis.

Thermal analysis was conducted to determine the behavior of the PCS web during pyrolysis. Figure 6 shows a comparison between the TGA results of the as-spun web, cured web, and as-received PCS. The as-received PCS showed weight losses at temperatures ranging from 400 to 700 °C and ceramic yields of approximately 65% Fig. 6(a). For the as-spun web shown in Fig. 6(b), a similar behavior was observed, except for some weight loss in the initial stage that might be caused by the evaporation of the solvent that remained after electrospinning. However, the cured web in Fig. 6(c) showed a delayed decomposition above 600 °C and the corresponding ceramic yield at 1000 °C was up to 92%, which was substantially higher than that of the as-spun web. This increased yield was also higher than that of the thermally-cured fiber prepared via melt spinning [26].

Figure 7 shows the DTG curves of the (a) as-received PCS, (b) as-spun web, and (c) cured web along with the

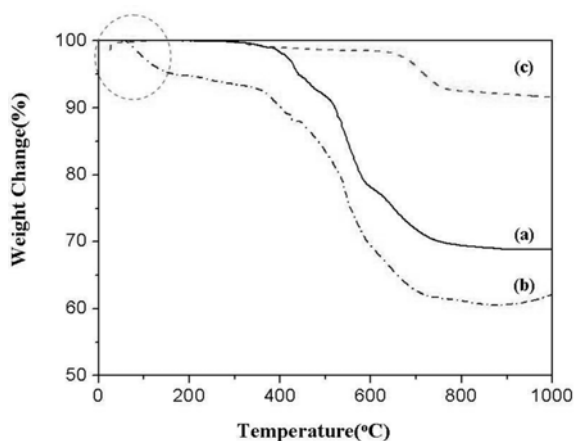


Fig. 6. TGA results of the (a) as-received PCS, (b) as-spun web, and (c) cured web.

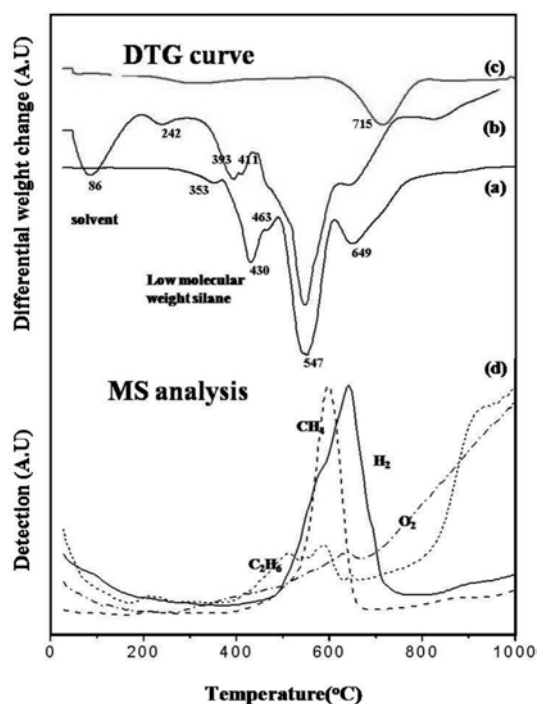


Fig. 7. DTG results of the (a) as-received PCS, (b) as-spun web, and (c) cured web in comparison to the mass analysis result of the (d) as-received PCS.

mass spectroscopy (MS) analysis of the (d) as-received PCS. The DTG curve of the as-received PCS Fig. 7(a) showed a weight reduction at 430 °C, 547 °C, and above 650 °C. These results corresponded well with the MS analysis, as shown in Fig. 7(d). The peak at around 547 °C appeared mainly due to CH₄ evolution, and the peak at around 650 °C appeared due to H₂ and O₂ evolution [26]. The peak at 430 °C was not coincident with the MS results; this peak is attributable to the evaporation of the PCS oligomer [26, 27]. The condensation of the oligomer is known to occur before its detection by the MS system [26, 27]. As for the as-spun web, the DTG curve showed the same tendencies as those for the as-received PCS, except for the peaks at approximately 86 °C due to the evaporation of the solvent. In contrast, there was only one significant weight loss for the cured web, as shown in Fig. 7(c). This is closely related to the H₂ or O₂ evolution but not to the CH₄ gas that might have been detected around 600 °C (see Fig. 7(d)). This result suggested that the curing process significantly changed the chemistry and bonding characteristics of the electrospun PCS fibers.

Figure 8 shows the FT-IR spectra of the as-spun web, cured web, and as-received PCS. For the as-received PCS, the characteristic absorption band at 2100 cm⁻¹ was related to the contribution of Si-H stretching, and bands at 1350, 1250 and 1410 cm⁻¹ were attributed to the CH₂ deformation in Si-CH₂-Si and the deformation in Si-CH₃. In the as-spun web, bands due to the residual solvent were observed at 1000-1500 cm⁻¹. The intensities of Si-H and Si-CH₃ bonds in the cured web were weaker

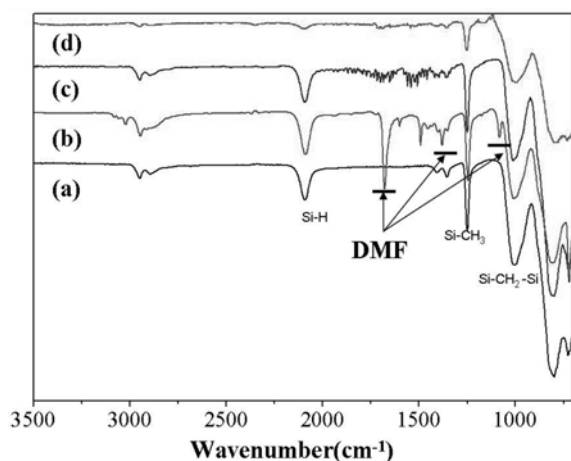


Fig. 8. FT-IR spectra of the (a) as-received PCS, (b) PCS solution (20% DMF/Toluene), (c) as-spun web, and (d) cured web.

Table 2. Chemical composition (wt%) of PCS web cured through (a) electrospinning and (b) melt spinning before curing

	Si	C	H	O
(a) Electrospun and cured web*	48.5	30.9	-	20.6
(b) Melt-spun and cured fiber ¹⁹⁾	53.9	32.5	0.1	13.5

*These values are estimated from the analysis results of EDS equipped with 400-kV HR-TEM.

than those of the as-received PCS. The absorption bands related to the Si-H and Si-CH₃ bonds are unique in PCS. These bonds can be easily exchanged with oxygen to form the Si-O-Si and Si-O-C bonds under specific conditions such as thermal oxidation cross-linking [28]. Therefore, the decrease in the intensity of the Si-H bond implies a high degree of cross-linking in the PCS. The FT-IR results indicated that large amounts of oxygen had been introduced into the web during thermal curing and this oxygen replaced the weakly bonded species such as hydrogen or methyl bonds as in the cross-linked portion, i.e., Si-O-Si or Si-O-C, of PCSs; this is also reflected in

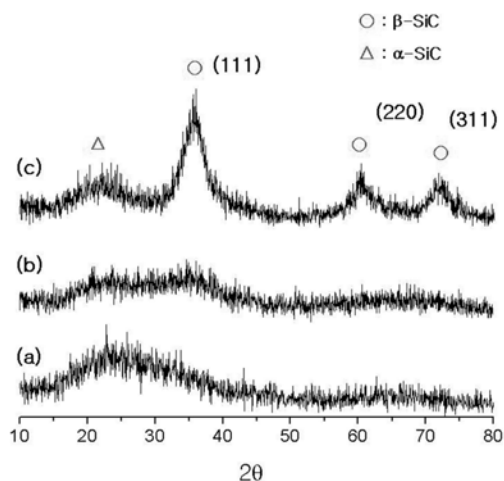


Fig. 9. XRD pattern for the SiC web sintered at (a) 1000, (b) 1200, and (c) 1400 °C.

the increased ceramic yield of 92% and compositions of the SiC web, as shown in Fig. 8(c) and Table 2.

Oxygen in the fiber affected the inorganic conversion behavior and furthermore the crystallization and high-temperature stability of the web. The XRD data for the SiC webs sintered at 1000, 1200, and 1400 °C are shown in Fig. 9. No peaks related to the SiC phase were detected for the web sintered at 1000 °C (Fig. 11(a)), except the broad peak corresponding to α -cristobalite at around 23°. At 1200 °C, the peak for (111) β -SiC appeared at around 35° along with the α -cristobalite peak, but the peaks were still broad and weak in their intensities. At 1400 °C, (111), (220), and (311) β -SiC peaks were observed with still broader peaks of α -cristobalite.

It is well known that during the pyrolysis at 1000–1200 °C, the PCS fiber is converted into inorganic phases of SiC nanocrystals and free carbon and the oxycarbide phase induced by oxidation curing [4, 29]. The SiC web with a large specific surface area will have a greater oxycarbide phase.

TEM images of the SiC web pyrolyzed at 1200 °C are shown in Fig. 10. The selected area diffraction pattern (SADP) of the small area of the fiber showed only a hollow ring, which indicates the glassy characteristics of the SiC fibers due to the large amount of the amorphous oxycarbide phase, α -cristobalite nanocrystals, and SiC nanocrystallites.

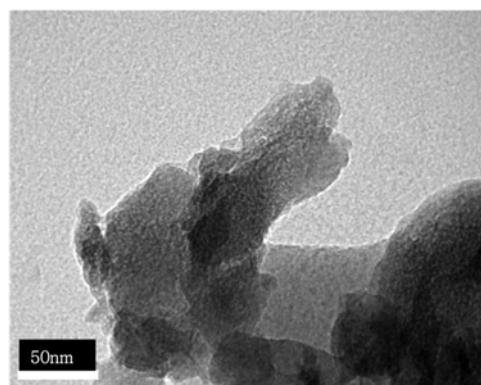
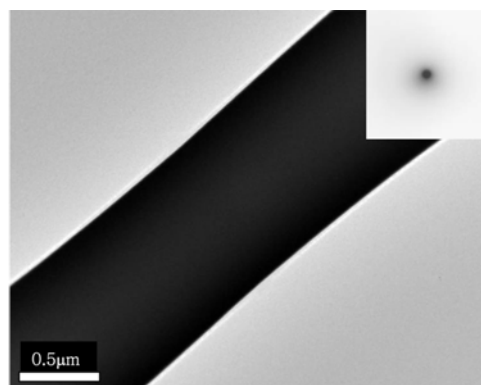


Fig. 10. TEM image at a voltage of 200 kV for the SiC web pyrolyzed at 1200 °C.

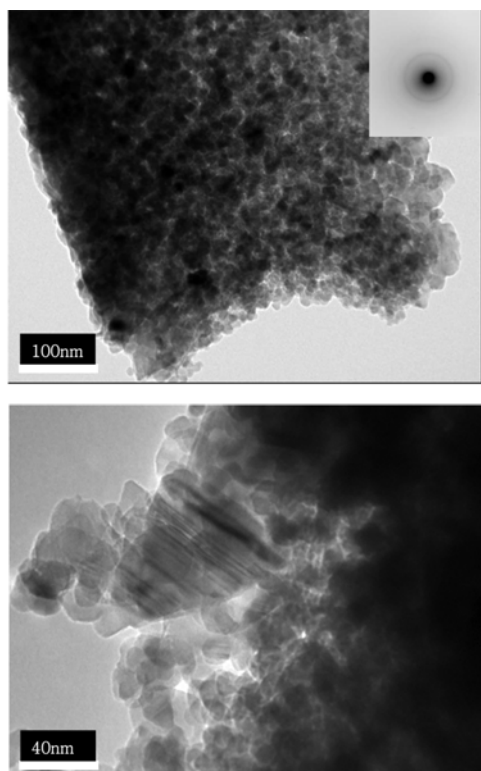


Fig. 11. TEM image at a voltage of 200 kV for the SiC web pyrolyzed at 1400 °C.

Figure 11 shows TEM images of the SiC web pyrolyzed at 1400 °C. The SiC crystals had coarsened and the fiber had a porous structure. Since oxycarbide phases are unstable at the high temperature of 1400 °C, they decompose into SiC nanocrystals, SiO and CO gas. This decomposition with some crystallization and the growth of nanocrystals without sintering rendered the fibers porous.

Conclusions

We have succeeded in fabricating an SiC web having intermediate fiber diameters of approximately 1-3 μm by a simple electrospinning and pyrolysis process. The spinnability, morphology, and diameter of the fibers were influenced by the solution concentration and solvent mixing ratio. DMF additions strongly affected the web formation, fiber-size reduction, web uniformity, and elimination of beads. The optimum spinning conditions to obtain a uniform SiC web were a 1.3 g/ml solution with 30% DMF/toluene composition and a spinning voltage higher than 20 kV. The as-spun web with a large specific surface area was drastically oxidized during the curing step, which resulted in an increase in the ceramic yields after pyrolysis. Oxygen also affected the conversion of the polymer phase to the ceramic phase and its final microstructure. A significant amount of cristobalite phase was observed together with SiC nanocrystallites and nanopores inside the fiber after the heat treatment at 1400 °C. This type of SiC web is expected to be potentially

applicable as a good catalyst support, a separator for thermal batteries, and for high-temperature particulate filters. A study of the mechanical properties, crystallinity, and stoichiometry of the highly crystallized SiC web and reduced oxygen content should be further explored.

References

1. Q.-M. Cheng, L.-V. Interrante, M. Lienhard, Q. Shen, and Z. Wu, *J. Euro. Ceram. Soc.* 25 (2005) 233-241.
2. P. Colombo, T.E. Paulson, and C.G. Pantano, *J. Am. Ceram. Soc.* 80[9] (2003) 2333-2340.
3. X. Bao, M.R. Nangerejo, and M.J. Edirisinghe, *J. Mater. Sci.* 35 (2000) 4365-4372.
4. A.R. Bunsell and M.H. Berger, *J. Mater. Sci. Lett.* (1995) 284-287.
5. D.H. Riu, Y. Kim, D.G. Shin, and H.R. Kim, *Ceramic Trans.* 154 (2003) 77-86.
6. D.G. Shin, D.H. Riu, Y. Kim, H.R. Kim, H.S. Park, and H. E. Kim, *J. Kor. Ceram. Soc.* 42[8] (2005) 593-598.
7. K. Schaupt, H. Wallau, M. Kahlke, and M. Kastel, US patent No. 5645411 (1997).
8. M.P. Henrichsen, W.C. Hakenkamp, and G.A. Mullins Jr, US Patent No. 6860917 (2005).
9. J. Adler, *Int. J. Appl. Ceram. Technol.* 2[6] (2005) 429-439.
10. R.A. Guidotti and F.W. Reinhardt, *Lithium Batteries* (2000) 772-780.
11. T.D. Kaun, *Power Sources Conference* (2004) 179-182.
12. S.Y. Gu, J. Ren, and Q.L. Wu, *Synthetic Metals* 155 (2005) 157-161.
13. Y. Wang, M. Aponte, N. Leon, I. Ramos, R. Furlan, and N. Pinto, *J. Am. Ceram. Soc.* 88[8] (2005) 2059-2063.
14. Y. Zhang, J. Li, Q. Li, L. Zhu, X. Liu, X. Zhong, J. Meng, and X. Cao, *Scripta Mater.* 56 (2007) 409-412.
15. D.T. Welna, J.D. Bender, X. Wei, L.G. Sneddon, and H.R. Allcock, *Adv. Mater.* 17[7] (2005) 859-862.
16. W. Sigmund, J. Yuh, H. Park, V. Maneratanana, et al., *J. Am. Ceram. Soc.* 89[2] (2006) 395-407.
17. A. Frenot and I. S. Chronakis, *Current. Opinion in Coll. Inter. Sci.* 8 (2003) 64-77.
18. I.S. Chronakis, *J. Mater. Proc. Tech.* 167 (2005) 283-293.
19. Z.M. Huang, Y.Z. Zhang, M. Kotaki, and S. Ramakrishna, *Comp. Sci. Tech.* 63 (2003) 2223-2253.
20. C.J. Buchko, L.C. Chen, Y. Shen, and D.C. Martin, *Polymer* 40 (1999) 7397-7407.
21. H. Fong, I. Chun, and D.H. Reneker, *Polymer* 40 (1999) 4585-4592.
22. J. Shawon and C. Sung, *J. Mater. Sci.* 39 (2004) 4605-4613.
23. C.M. Hsu and S. Shivkumar, *Macromol. Mater. Eng.* 289 (2004) 334-340.
24. K.H. Lee, H.Y. Kim, Y.M. La, D.R. Lee, and N.H. Sung, *J. Poly. Sci. B: Polymer Physics* 40 (2002) 2259-2268.
25. S.H. Park, C. Kim, and K.S. Yang, *Synthetic Metals* 143 (2004) 175-179.
26. G. Chollon, M. Czerniak, R. Pailler, X. Bourrat, R. Naslain, J.P. Pillot, and R. Cannet, *J. Mater. Sci.* 32 (1997) 893-911.
27. E. Bouillon, F. Langlais, R. Pailler, R. Naslain, F. Curege, P.V. Huong, J.C. Sarthou, A. Delpuech, C. Laffon, P. Lagarde, M. Monthieux, and A. Oberlin, *J. Mater. Sci.* 26 (1991) 1333-1345.
28. H.Q. Li, R. Taylor, R.J. Day, and F. Heatler, *J. Mater. Sci.* 36 (2001) 4037-4043.
29. H.Q. Li, R. Taylor, R.J. Day and F. Heatler, *J. Mater. Sci.* 36 (2001) 4045-4057.